Serbian Tribology Society

SERBIATRIB '25

19th International Conference on Tribology

Faculty of Engineering University of Kragujevac

Kragujevac, Serbia, 14 – 16 May 2025

Research paper DOI:10.24874/ST.25.121

VISCOMETRY ON SYNTHETIC AND FULLERENE BASED OILS AND A CFD INVESTIGATION ON COMPRESSION PISTON RING

Elias TSAJIRIDIS[1], Alexandra ANYFANTI[1], Pantelis NIKOLAKOPOULOS[1,*]

[1]Mechanical Engineering and Aeronautics Department, University of Patras, Greece

*Corresponding author: pnikolakop@upatras.gr

Abstract: *Nowadays, for the highly efficient engines, a comprehensive assessment of all tribological parameters that influence their performance is significant. Among these, the friction and wear which remain critical parameters of interest, focusing on strategies in order to minimize them. This work, investigates the use of nanoparticles to enhance the rheological properties of lubricants, specifically employing C60 fullerenes as additives, in compression piston ring-cylinder liner interfaces. Experimental measurements of lubricant viscosity, including synthetic oil and fullerene-based oils, were tested using a capillary tube viscometer, under varying temperature and pressure conditions. The obtained viscosity diagrams and the respective uncertainty analysis have been presented in detail for every lubricant tested. The experimentally obtained viscosity values are used as inputs into a computational fluid dynamic (CFD) model of the cylinder-compression piston ring tribological system. The analysis explores the effect of surface asperities on friction, lubricant film formation, and hydrodynamic pressure. Additionally, the study incorporates the influence of temperature variations throughout the engine's four-stroke cycle on the lubricant's rheological properties. The phenomenon of cavitation, occurring under high compression conditions, is also examined, with its influences on engine performance. Engine performance comparisons, between synthetic and fullerene C60 enhanced oils, have been depicted, and results presented.*

Keywords: *lubricant, C60 fullerene, cavitation, viscosity, piston ring tribology*

1. INTRODUCTION

The pursuit of enhanced engine efficiency has driven a reduction in lubricating oil viscosity, aimed at minimizing losses within hydrodynamic lubrication mechanisms. This approach has, in turn, elevated the significance of piston ring and cylinder bore systems in managing mixed and boundary lubrication scenarios. To optimize friction efficiency in the certain lubrication regimes, one of the strategies involves the application of friction modifiers [1,2].

Synthetic lubricants frequently incorporate nanoparticles as additives, which come in varying dimensions, forms, and volume ratios. In numerous tribological applications, lubricants enriched with nanoparticles, have demonstrated superior performance in terms of reducing friction and wear. This improvement can be attributed to their exceptional dispersion properties, enhanced lubricating characteristics, and improved thermal conductivity.

Consequently, gaining a comprehensive understanding of nanoparticle behavior is imperative for advancing mechanisms of lubrication, which, in its turn, can aid in meeting stringent regulations governing vehicle emissions [1]. Underscored the increasing significance of the tribofilm creation is initiated by friction modifiers and antiwear additives at the contact interface. This effect proves especially advantageous in mitigating frictional losses and reducing energy consumption, particularly with the realm of transportation. Notably, these advantages become most apparent in situations where the oil film is limited, as in mixed and boundary lubrication scenarios [2]. To attain reduced friction and wear in various mechanical interactions, a variety of nanoparticle types, typically ranging from 1 to 120 nanometers in size, are introduced into diverse lubricants.

In the piston ring- cylinder liner conjunction where the lubricant flow in mixed lubrication regime, it is crucial to investigate how the friction and the wear as well, could be minimized. Using fullerene enhanced lubricants is of great interest, as previous works highlight their great significance in improving engine's performance [3]. The viscosity is the main reason for a lubricant to be selected. In the case of a low viscosity, the lubricant film would not the expected or desired thickness, and on the other hand, if the viscosity is higher from the requested one, it impedes motion by increasing resistance. The viscosity though isn't a steady state property, as it takes different values according to temperature and pressure as well. In this research the viscosity of the monograde lubricant SAE30 and one using fullerenes as additives is investigated and computed experimentally. The viscosity measurement tests were performed using an EH105 capillary tube viscometer manufactured by DELTALAB.

The temperature range varied between 25°C to 80 °C and the pressure was up to 2 MPa.

The viscometer and its main parts are presented in Figure 1. The fluid under examination is introduced into the pressurized chamber (1) and secured onto the magnetic stirring device (15). Pressure is introduced into the tube (3) at a level regulated by the control valve (11) and observed using the mercury pressure gauge (12). The capillary tube is positioned within the temperature-controlled sleeve (2). Both this sleeve and the coil (5), placed inside the chamber, are supplied with water maintained at a constant temperature by the control unit (8). The fluid moves through the capillary tube at the temperature recorded by the thermometer and then flows into the calibrated pipette (14). The button (13) releases compressed air into the calibrated pipette. The chamber can be emptied via the outlet nozzle (6). By determining the time required to fill the calibrated pipette, the fluid's viscosity is calculated in relation to the temperature.

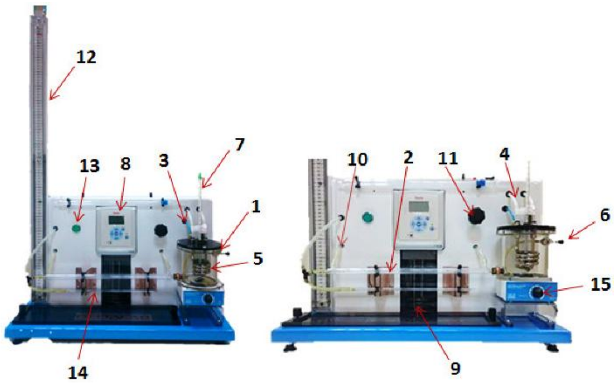

Figure 1. The Eh105 capillary tube viscometer

Measuring the rheological properties of a lubricant is a chalenging task. The capability to assess viscosity across various flow rates, and consequently shear rates, inherently requires rheometric functionality. Viscometers such as cone and plate and coaxial cylinder ones are better suited for obtaining measurements at higher shear rates. The priority here, was given to the fullerene enhanced lubricant, which is of great interest considering that using such a lubricant, improves engine's environmental footprint in terms of emissions. The viscosity of SAE 30 is also measured, used also for validation purposes, as it had been measured previously by Mavroudis et al. [4], using the same viscometer.

A two-dimensional computational fluid dynamics (CFD) model is developed using Ansys FLUENT. The flow problem is nonlinear, with the governing equations being interconnected. The pressure-based mixture model is employed, and the velocity-pressure coupling is addressed using the

Semi-Implicit Method for Pressure-Linked Equations (SIMPLE) algorithm. The SIMPLE algorithm minimizes errors caused by discretization, incorporating a second-order upwind scheme. Grid sensitivity analyses are conducted to identify optimal mesh specifications. In this case, a total of 31,031 quadrilateral elements are employed. Additionally, a time step of 10^{-3} seconds is selected to ensure flow stability during the simulation. A convergence criterion of 10^{-5}, in respect to pressure, has been applied. The viscosity is modeled using the power-law approach, as explained by Zavos and Nikolakopoulos [5], as the thermal transfer as the lubricant flows has been considered. The compression piston ring cylinder conjunction is presented schematically below in Figure 2.

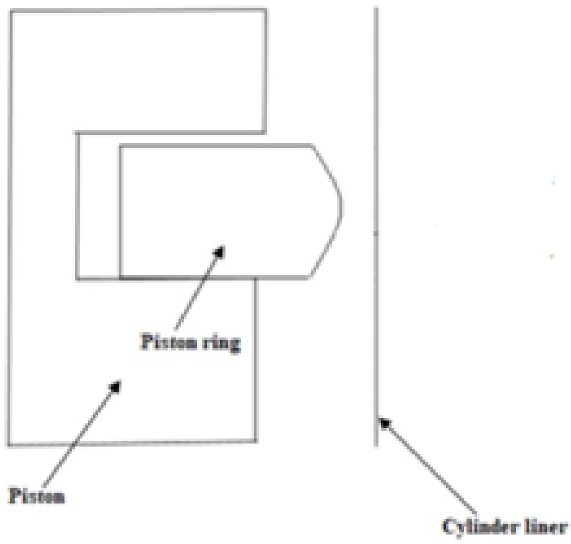

Figure 2. Compression piston ring cylinder conjuction

2. MEASUREMENT METHODS AND CFD MODEL

Apart from the thermal considerations, a UDF code (User Defined Function) is employed, so the asperities are regarded and affect the lubricant flow as per Greenwood and Tripp model [6]. Addiotionally, the cavitation phenomena are examined, trying to investigate whether and up to which area of the lubricant using fullerene additives is showing a better perfomance. The rheological properties of the fullerene based lubricant are well improved, as per Tsakiridis and Nikolakopoulos [3].

2.1 Theory of the elastodynamics of the piston ring

The piston's sliding velocity has a vital effect on the movement of the piston. This velocity is calculated by Equation (1):

$$v_{ring} \approx v_p = r_{cr}\omega(\sin\varphi + \frac{\lambda_{cr}}{2}\sin 2\varphi) \quad (1)$$

where:

- 'r' is the radius of the crankpin.
- 'ω' is the rotational speed of the engine.
- 'φ' represents the crank angle.
- 'λ_{CR}' is the control ratio.

As explained and analysed in [4] the ring profile is considered as parabolic, with an equation of $\frac{cx^2}{(\frac{b}{2})^2}$. In reality, the ring profile has a rough axial asymmetric shape as reported in [7]. In the following Figure 2, the loads and pressures exerted on the ring are presented during both the downstroke and the upstroke. As observed, there is no change in the direction of the forces. However, the pressure direction changes depending on whether the piston is moving towards Top Dead Center or Bottom Dead Center.

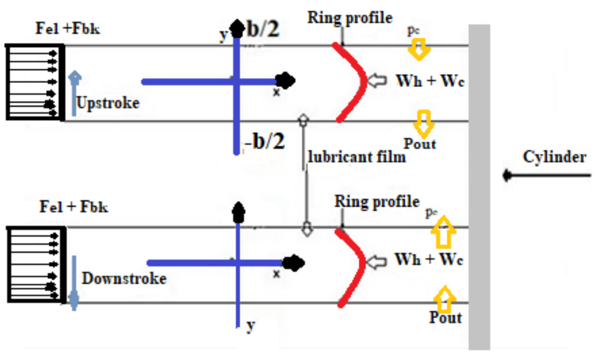

Figure 3. Boundary conditions and forces at ring-cylinder conjunction

The gas pressure at the back of the ring is determined by considering the primary forces depicted in Figure 1, which are summarized as below. Firstly, the back-gas force is given by the following equation:

$$F_G = 2\pi r_0 b_{pk}(\varphi) \qquad (2)$$

Moreover, the tension force of the ring is defined as follows:

$$F_T = 2\pi b r_0 p_{el} \qquad (3)$$

and the pressure due to elasticity is obtained as per Equation (4):

$$p_{el} = \frac{d_{gap} E_r \frac{bd^3}{12}}{3\pi b (\frac{d_{cyl}}{2})^4} \qquad (4)$$

where d_{gap} represents the piston-ring end gap and d_{cyl} stands for the cylinder bore diameter. In the present analysis, it is imperative that the ring tension force F_T summarized with the back-gas force F_G are balanced with the hydrodynamic reaction W_h generated by the lubricant film in the ring–liner interface, adding the load stemming from surface irregularities, denoted as W_C. The balance of the ring must be maintained at every crankshaft angle, as per the following expression:

$$F_T + F_G = W_h + W_C \qquad (5)$$

In both mixed and hydrodynamic lubrication regimes, the contact in the ring-cylinder interface is not completely insulated by the film of the lubricant. Instead, a section of the ring contacts surface asperities. The local hydrodynamic capacity and the load by the surface asperities are calculated by the following equations:

$$W_h = 2\pi r_0 \int b_0 p_h dx dy \qquad (6)$$

$$W_C = \frac{16\sqrt{2}}{15} \pi (\zeta \kappa \sigma)^2 \sqrt{\frac{\sigma}{\kappa}} \frac{E' A F_5}{2(\lambda)} \qquad (7)$$

Load balance is put over when the Equation (8) is checked up:

$$X = \frac{|W(\varphi) - F(\varphi)|}{\max\{F, W\}} \leq 0.1\% \qquad (8)$$

The motion of the fullerene particles as the lubricant flows in the ring-cylinder conjuction, is described by Tsakiridis and Nikolakopoulos [3]. The particles prevent the surfaces from having direct contact by rolling between them, even in the case that the lubricant film isn't sufficient, as in this case the lubricant is empoyed in mixed lubrication regime.

2.2 Method of viscosity measurements using capillary tube viscometer

The experimental procedure for the viscosity measurement of engine oils is described step by step in Figure 4. The dynamic viscosity (n) is defined as:

$$n = \frac{\Delta p}{q} \frac{\pi R^4}{8l} \qquad (9)$$

where R is the capillary tube radius, l is the capillary tube length, and $\frac{\Delta p}{q}$ is the gradient from the line defined, figuring the variation of Δp versus q.

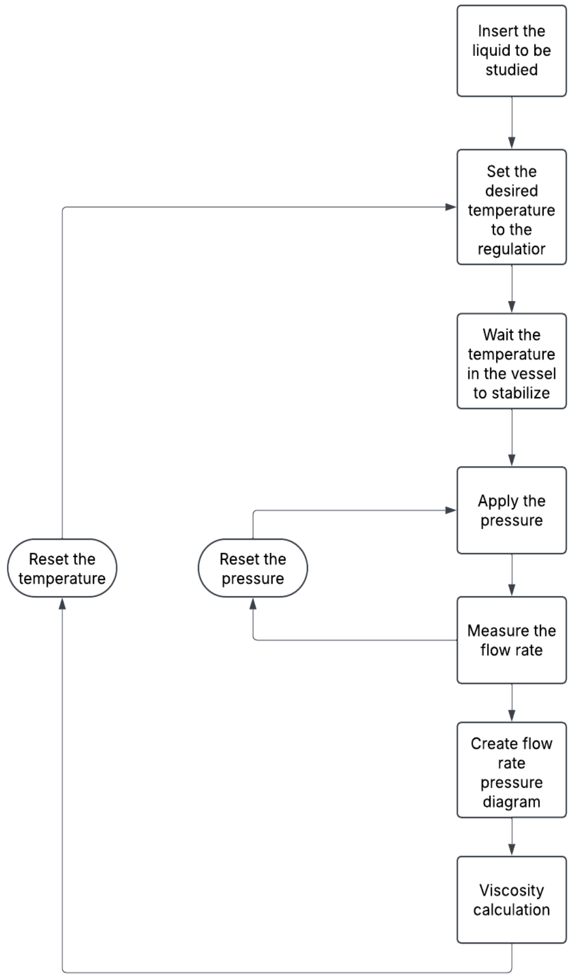

Figure 4. The flowchart describing the viscosity measurements

Upon receiving a set of flow rate measurements, the values were plotted against their corresponding pressures. To confirm that the flow is indeed Poiseuille flow, the experimental data points should align with a straight-line equation.

2.3 Uncertainty analysis

Regarding the process followed by this specific device, the following parameters are necessary for the uncertainty analysis:

- Uncertainty in pressure measurement, $u_{\Delta p}$
- Uncertainty in flow rate measurement, u_q
- Uncertainty in volume measurement, u_v
- Uncertainty in time measurement, u_t
- Uncertainty from the radius of the capillary tube, u_r
- Uncertainty from the length of the capillary tube, u_l

Since all the above input quantities are independent, the square of the standard deviation of the output estimate yy is given by the following equation:

$$u^2(\eta) = \sum_{i=1}^{n}[c_i * u(x_i)]^2 = \sum_{i=1}^{n} u_i{}^2(\eta) \quad (10)$$

Table 1. Uncertainty parameters and their values

Parameter(x_i)	Value u(x_i)
Δp	0.5 mmHg
V	0.005ml
T	0.01s
L	0.0025 mm
R	0.05 mm

So, the uncertainty equation is:

$$u^2(\eta) = \sum\left(\frac{\theta\eta}{\theta(\Delta p)}u(\Delta p) + \frac{\theta\eta}{\theta(V)}u(V) + \frac{\theta\eta}{\theta(t)}u(t) + \frac{\theta\eta}{\theta(l)}u(l) + \frac{\theta\eta}{\theta(R)}u(R)\right)^2 =$$

$$\sum\left(\frac{\pi R^4}{q\,8\,l}\mathrm{u}(\Delta p) - \frac{\Delta p\,\pi R^4 t}{8\,l}\frac{1}{V^2}u(V) + \frac{\Delta p\,\pi R^4}{V\,8\,l}u(t) + \frac{\Delta p\,\pi R^3}{q\,2\,l}u(R) - \frac{\Delta p\,\pi R^4}{q\,8\,l^2}u(l)\right)^2 \quad (11)$$

And by calculating for all the measurements taken at different temperatures and pressures, we conclude that:

$$u^2(\eta) = 0{,}001698167$$

The combined uncertainty is derived from the positive square root of the variance:

$$u_c(\eta) = \sqrt{u_\eta{}^2} = 0{,}041208$$

The uncertainty assigned to each result should be of an appropriate range so that it covers an interval with a high degree of confidence (increasing the probability of the result's correctness). So,

$$U = k * u_c(y) = 2 * 0{,}041208 = \mathbf{0,082416}$$

2.4 Cavitation model analysis

The CFD model of the lubricant flow is deployed using ANSYS FLUENT, considering thermal transfer between the surfaces and the lubricant, the Greenwood-Tripp model and the cavitation phenomena as well.

The cavitation phenomena were modelled deploying two phases as a mixture, the liquid and the vapor phase, and the fullerenes were deployed by using the discrete phase model. With this model the liquid-vapor mixture is homogenous but, on the other hand, the lubricant-fullerenes mixture is non-homogenous. In Table 2 the parameters of the cavitation model are presented.

Table 2. Cavitation parameters for the CFD model

Parameter	Symbol	Units	Value
Vaporization Pressure	P_v	Pa	$2*10^4$
Atmospheric Pressure	P_{atm}	Pa	101.325
Lubricant density in vapor phase	ρ_g	Kg/m^3	1,2
Bubble's diameter	D_b	m	$2*10^{-5}$
Lubricant viscosity in vapor phase	μ_g	Pas	10^{-5}

These values for the cavitation model used for the analysis, while the lubricant used is SAE 30. The lubricant properties are well described and analysed by Zavos [8]. This research was used for validation of the results obtained from this model.

The piston ring speed as well as the chamber pressure, for every angle of the crankshaft, are used as boundary conditions in our CFD model. Piston ring velocity for an engine operating at 1500 rpm and 50% throttle is presented, as well as the chamber pressure for every crank angle are presented in [4].

Recent research by Gore et al. [9] and Söderfjäll et al. [10] has significantly focused on analyzing the piston ring interface, integrating numerical predictions with well-validated direct measurements. Notably, the geometry and surface roughness of the ring can significantly affect lubrication mechanisms, especially in mixed and hydrodynamic regimes. Previous studies [11] have demonstrated that these effects can vary by 5–25%, depending on operational conditions. The key contribution of this study is its exploration of how nanoparticle-enhanced lubricants influence this system, utilizing an advanced CFD model to deepen our understanding of this intricate interaction.

3. RESULTS

3.1 Capillary tube viscometer results

Before measuring the viscosity of the lubricant using fullerene additives it was crucial to validate the results obtained. So, firstly the procedure was done for SAE 30 lubricant, at 60°C, 70°C and 75°C, and the viscosity values were compared to Nikolakopoulos et.al [4], and the divergence was negligible. Following the procedure was done for the fullerene lubricant and the relevant results are presented below. The pressure was set to 100mm Hg, 200 mm Hg and 300 mm Hg respectively.

As shown in the figure above, viscosity decreases as temperature increases, which is consistent with expected behavior. Additionally, pressure has a significant influence on viscosity; as pressure rises, viscosity also increases. To highlight the critical role of fullerenes in modifying the rheological properties of the lubricant, Figure 6 below presents viscosity curves comparing the fullerene-enhanced lubricant with a conventional SAE 30 lubricant.

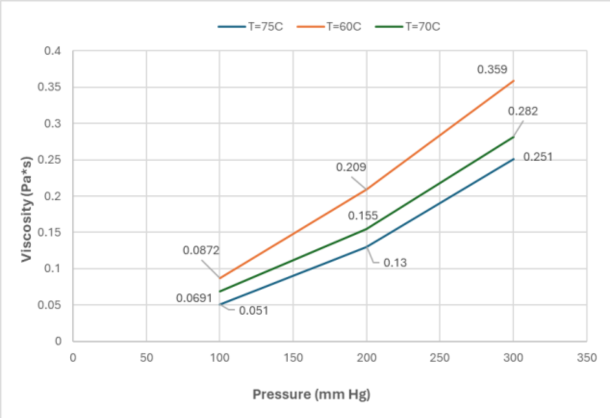

Figure 3. Viscosity of fullerene lubricant at various pressures and temperatures

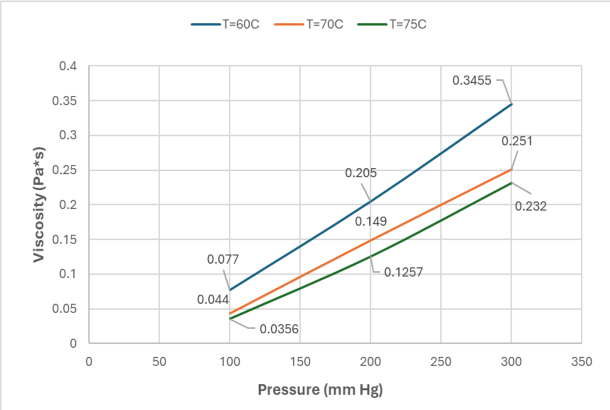

Figure 4. Viscosity of SAE 30 lubricant at various pressures and temperatures

The viscosity of the lubricant containing fullerenes as additives increases and maintains its properties even as the temperature rises. While viscosity typically decreases with increasing temperature, the fullerene-enhanced lubricant demonstrates significantly less degradation compared to conventional monograde oil. This is a critical advantage, as engines often operate under high-temperature conditions, and maintaining sufficient lubricant viscosity, is essential for optimal engine performance and protection.

3.2 Cavitation model results

By using the CFD model a study of the tribological performance of the two lubricants was done, considering the cavitation and computing the volume of fraction of the vapor phase.

For the validation of the results, before proceeding to the investigation, there were used the boundary conditions described in [8], and the results obtained were compared. In Figure 5 the validation diagram is presented.

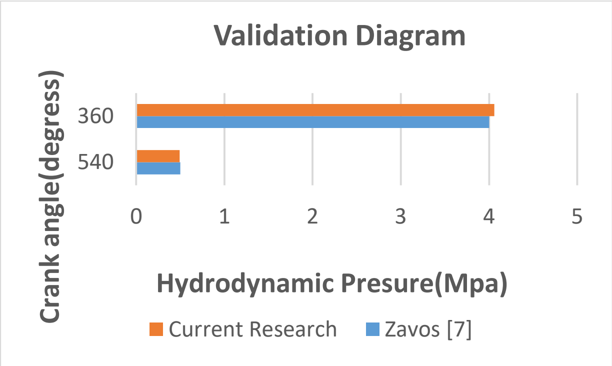

Figure 7. Validation diagramm

The hydrodynamic pressure is computed at two different angles, -180° and 360° of the crankshaft and the difference is predicted up to 3%. So, the results are robust, and the investigation is proceeding further for the fullerenes lubricant. The results obtained for the lubricant containing fullerenes are compared with the ones for the SAE 30. The results obtained in terms of hydrodynamic pressure and volume fraction of the vapor phase are presented and analysed.

In the following figures, there is a comparison between the hydrodynamic pressure exerting on the piston ring along with the volume fraction of the vapor phase at -180°, as the two lubricants flow.

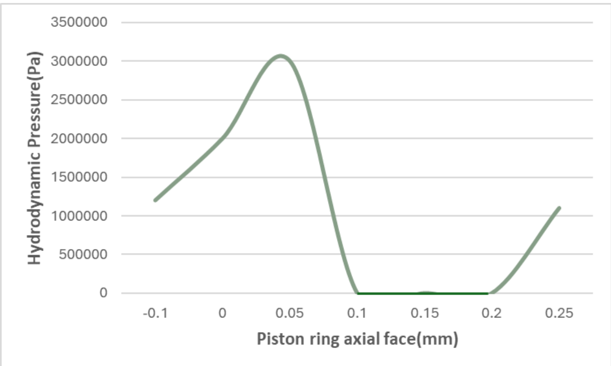

Figure 6. Hydrodynamic pressure at -180° for the fullerene lubricant along the piston ring profile

As obtained from the above figures, the volume fraction of the vapor phase is well increased when the lubricant using fullerenes additives is deployed. That's beacause of the nano particles which enhance the cavitation phenomena. These nanoparticles can act as nucleation sites for cavitation bubbles, increasing the cavitation intensity in the lubricant film.

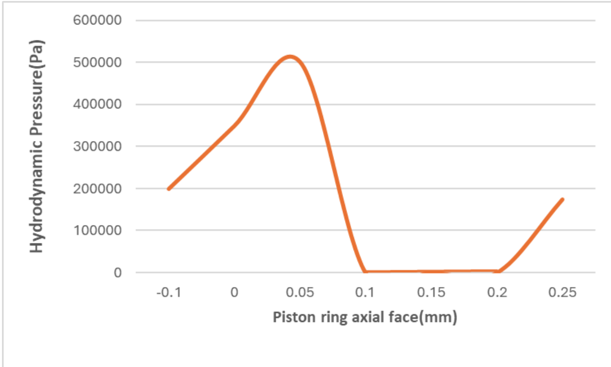

Figure 7. Hydrodynamic pressure at -180° for the SAE 30 along the piston ring profile

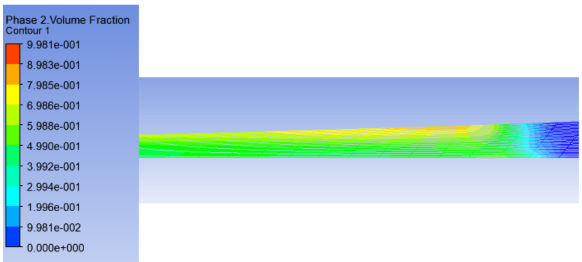

Figure 8. Volume of fraction of the vapor phase at -180° for the fullerene lubricant

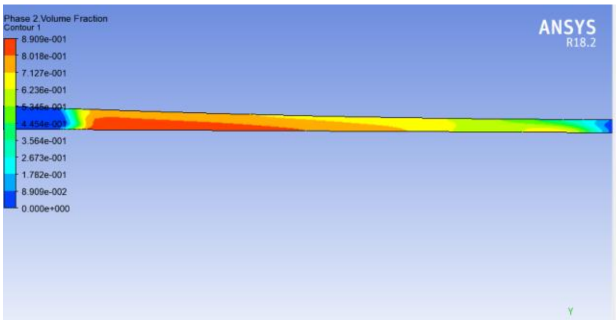

Figure 9. Volume of fraction of the vapor phase at -180° for the SAE 30 lubricant

On the other hand, the pressure is increased when the fullerene oil is deployed. In mixed lubrication regime, where the thinner lubricant film causes increased hydrodynamic pressure, this is expected. The lubricant containg fullerenes corresponds to lower lubricant films as per[3], since the particles enhance the rheological prperties of the lubricant.

In the following figures the same comparison, in terms of volume fraction and hydrodynamic pressure, is presented at 360°. At -180° the piston is near the Top Dead Center, but at 360° it is near the Bottom Dead Center, so another comparison can be done of how the two lubricants correspond at these two different positions.

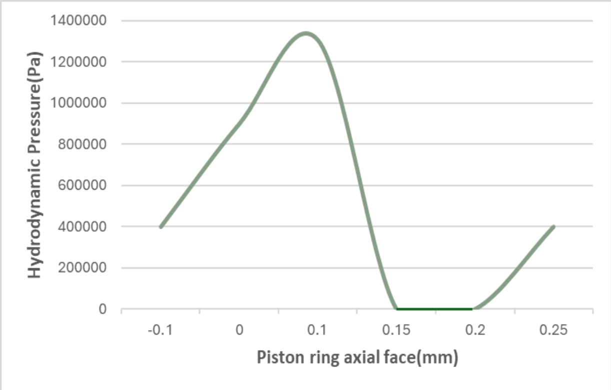

Figure 10. Hydrodynamic pressure at 360° for the fullerene lubricant along the piston ring profile

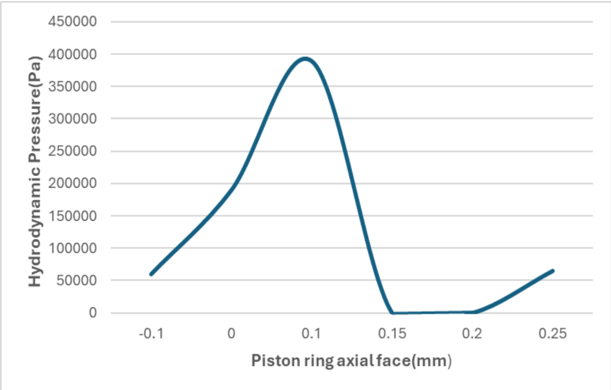

Figure 11. Hydrodynamic pressure at 360° for the SAE 30 along the pisron ring profile

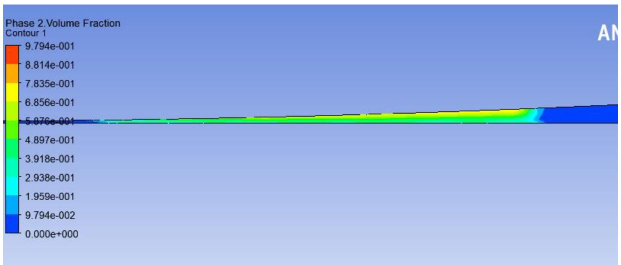

Figure 12. Volume of fraction of the vapor phase at 360° for the fullerene lubricant

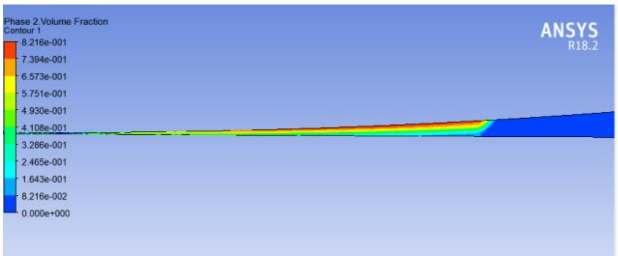

Figure 13. Volume of fraction of the vapor phase at 360° for the SAE 30 lubricant

The figures above (8,9,12,13) illustrate the hydrodynamic pressures that are generated, along with the vapor volume fraction (10,11,14,15), during the stroke reversals. As obtained at -180° the volume of fraction, Figure 10 and Figure 11, and the hydrodynamic pressure, Figure 8 and Figure 9, are well increased when using the lubricant containing fullerenes. It is clear that under high load and low speed conditions, particularly during the transition from the compression to the power stroke near top dead center (TDC), the contact area between the ring profile and the cylinder liner has been expanded. This occurs because the ring moves upward slowly at TDC (ϕ = -180°). Conversely, as the piston moves downward after the power stroke and approaches bottom dead center (BDC) (ϕ = 360°), the contact area of the ring reduces. This reduction is due to the lower load and the presence of an adequate minimum film thickness, supported by higher lubricant viscosity under isothermal conditions.

Additionally, the viscous friction is of great interest, and in Figure 16 is obtained the vital role that fullerenes play in improving the properties of the lubricant. Although the hydrodynamic pressure is increased, as well as the volume fraction of the vapor phase, on fullerenes oil state, the viscous friction is well decreased, Figure 16. The decreased friction results reflects also in decreased wear volume and further it improves the engine's operation.

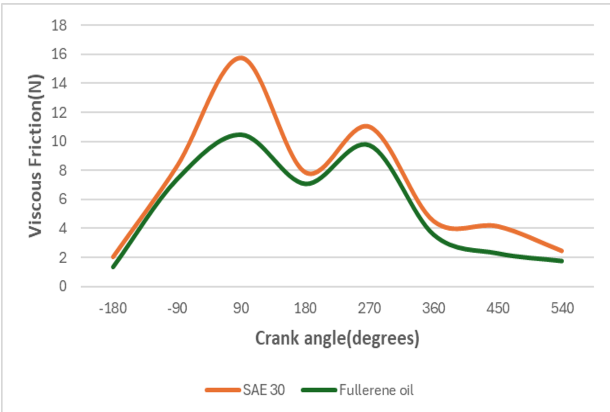

Figure 14. Viscous friction of lubricant SAE 30 and the lubricant containg fullerenes

4. CONCLUSIONS

A CFD model is developed to study the effect of lubricants containing fullerenes against SAE30 lubricant oils, regarding the tribology of the piston ring problem. It is obtained that the fullerenes well improve the rheological properties of the lubricant. In terms of hydrodynamic pressure, the lubricant containing fullerenes as additives corresponds to higher values of pressure. It is explained by the fact that the lubricants operate at mixed lubrication regime, and as a result, higher film thickness causes higher pressure. The minimum film thickness is well decreased when the fullerene oil is deployed as per [3], and so the hydrodynamic pressure is increased by almost 70% at -180° and by almost 80% at 360°. This increase in terms of hydrodynamic pressure is a result of the decrease of the minimum lubricant film that occurs when the lubricant containing fullerenes is deployed, and since the lubrication regime is the mixed one [3,5,8]. On the other hand, the viscous friction shows a decrement of almost 35% in maximum value at 90^0, which highlights the influence of the particles.

The experimentally measured viscosity indicates that the lubricant containing fullerenes as additives exhibits significantly improved performance, since the fulleneres additives do really enhnace the rheological properties of the lubricant [3]. Unlike lubricant SAE 30, the viscosity of fullerene enhanced lubricant remains more stable as the temperature increases, demonstrating a higher viscosity index, as per Figure 5. More speicifically, for pressure 100 mmHg the viscosity of Sae 30 when the temperature rises from 60°C to 70°C indicates a decrease of 42%, while the fullerene oil only 20%. Additionally, for 300 mmHg pressure, when the temperature follows the same increase, the decrease of viscosity is 27% for SAE 30 and 21% for fullerene oil. This also highlights the great influence of fullerene particles, since the decrease in viscosity is almost the same for the two pressure regimes while for SAE 30 the decrease is way bigger at low pressure. Furthermore, the fullerene-based lubricant not only performs better with temperature variations but also maintains superior stability under pressure changes. The maximum increase is obtained for both lubricants, for temperature of 70°C. Specifically, SAE 30 increases its viscosity when the pressure increases from 100mmHg to 200 mmHg about 70%. Respectively, the viscosity of the fullerene oil increases 55% at the same time. The maximum difference in viscosity values between the two lubricants is obtained at 70°C and pressure 100 of mmHg, which is about 35%.

ORCID iDs

Elias TSAJIRIDIS 0009-0008-1322-9134
Alexandra ANYFANTI 0009-0005-6540-5759
Pantelis NIKOLAKOPOULOS 0000-0002-0944-6653

REFERENCES

[1] H. Spikes, “Friction modifier additives,” Tribology Letters, vol. 60, no. 5.167, Jun. 2017, doi: 10.24874/ti.2017.39.02.02.
[2] L. S. Rudnick, Lubricant Additives—Chemistry and Applications, 2nd ed., Boca Raton, FL, USA: CRC Press, 2009.
[3] E. Tsakiridis and P. Nikolakopoulos, “Fullerene oil tribology in compression piston rings under thermal considerations,” Lubricants, vol. 11, no. 12, p. 505, 2023, doi: 10.3390/lubricants11120505.
[4] P. G. Nikolakopoulos, S. Mavroudis, and A. Zavos, “Lubrication performance of engine commercial oils with different performance levels: The effect of engine synthetic oil aging on piston ring tribology under real engine conditions,” Lubricants, vol. 6, no. 4, p. 90, 2018, doi: 10.3390/lubricants6040090.
[5] A. Zavos and P. G. Nikolakopoulos, “A tribological study of piston rings lubricated by power law oils,” Proceedings of the Institution of Mechanical Engineers, Part J: Journal of Engineering Tribology, vol. 230, pp. 506–524, 2016.
[6] J. A. Greenwood and J. H. Tripp, “The contact of two nominally flat rough surfaces,” Proceedings of the Institution of Mechanical Engineers, vol. 185, pp. 625–633, 1970.
[7] W. Ma, N. Biboulet, and A. A. Lubrecht, “Performance evolution of a worn piston ring,” Tribology International, vol. 126, pp. 317–323, 2018.
[8] A. Zavos and P. G. Nikolakopoulos, “Cavitation effects on textured compression rings in mixed

lubrication," Lubrication Science, vol. 28, pp. 475–504, 2016, doi: 10.1002/ls.1341.

[9] M. Gore, R. Rahmani, H. Rahnejat, and P. King, "Assessment of friction from compression ring conjunction of a high-performance internal combustion engine: A combined numerical and experimental study," Proceedings of the Institution of Mechanical Engineers, Part C: Journal of Mechanical Engineering Science, vol. 230, pp. 2073–2085, 2016.

[10] M. Söderfjäll, A. Almqvist, and R. Larsson, "Component test for simulation of piston ring–cylinder liner friction at realistic speeds," Tribology International, vol. 104, pp. 57–63, 2016.

[11] M. Kennedy, S. Hoppe, and J. Esser, "Lower friction losses with new piston ring coating," MTZ Worldwide, vol. 75, no. 4, pp. 24–29, 2014